Dalton Transactions

Accepted Manuscript

ROYAL SOCIETY OF CHEMISTRY

www.rsc.org/dalton

Journal Name

COMMUNICATION

Simultaneous observation of ligand-based fluorescence and phosphorescence within a magnesium-based CP/MOF at room temperature

Received 00th January 20xx,
Accepted 00th January 20xx

DOI: 10.1039/x0xx00000x

www.rsc.org/

Lu Zhai,[a, b] Wen−Wei Zhang,*[b] Jing−Lin Zuo,[b] Xiao−Ming Ren*[a,b,c]

A highly thermal stable CP/MOF, comprised of Mg^{2+} and H_2EBTC^{2-} with a formula of $[Mg(H_2EBTC)(DMF)_2]$, emits dual band luminescence centered at 376 and 555 nm. The former is assigned to fluorescence of H_2EBTC^{2-} and the later with 1.63 µs decay lifetime and large Stokes shifts corresponds to phosphorescence of H_2EBTC^{2-}. To the best of our knowledge, this is the first time to observe the ligand-based phosphorescence in a CP/MOF without any heavy atom at room temperature.

Over the past two decades, coordination polymers (CPs) or coordination networks (CNs), also called metal-organic frameworks (MOFs), have received growing interest due to their widely potential applications, ranging from gas storage,[1] catalysis,[2] optics,[3] proton conductor,[4] fluorescence sensor[5] to biomedical imaging or drug delivery.[6] Moreover, with respect to conventional inorganic matters, the CPs/MOFs have distinctive advantages owing to their special incorporation of inorganic and organic building blocks, tunable highly ordered structures, and their facile synthesis routes.

In the context of luminescent materials, the phosphorescent CPs/MOFs are of particular increasing interest due to their practical applications in the fields of organic light-emitting diodes (OLEDs),[7] light-emitting electrochemical cells,[8] biolabeling,[9] chemosensors[10] and oxygen sensor,[11] as well as time-resolved fluoroimmunoassay (TRFIA) analysis.[12] The phosphorescent emission in a conjugated organic molecule concerns the intersystem crossing process, and this is a non-radiative energy transfer process from the first excited singlet state (S_1) to the first excited triplet state (T_1) and can be assisted by spin-orbit coupling, vibration coupling or the presence of paramagnetic ions. Many CPs/MOFs based on either the heavy-metal ions (e.g., Ir, Ru, Os, Pt)[13, 14] or lanthanide ions[15] emit intense phosphorescence owing to the existence of strongly spin-orbit coupling interactions within the heavy-metal ions or lanthanide ions. It has been also observed that lots of aromatic carboxylate ligands show weak or no intraligand $\pi\leftarrow\pi^*$ transition fluorescence in solid state due to the formation of excimers, which is due to the strong $\pi\cdots\pi$ stacking between aromatic rings. Generally, an excimer relaxes to the ground state by non-radiative process, which leads to the luminescence quenching; otherwise, the CPs/MOFs display intense aromatic carboxylate ligand-based fluorescence in the cases of the presence of no $\pi\cdots\pi$ stacking between the aromatic rings in the neighboring ligands.[16] Noticeably, it has been seldom reported that an organic compound or coordination compound only containing light-atom emits phosphorescence in solid state, especially at ambient temperature.

In general, there is no spin-orbit coupling in a compound comprised of main-group light elements, however, it is possible that such a compound emits phosphorescence by the vibration coupling-assisted intersystem crossing process. Herein, we present a fascinating example that a CP/MOF, built only from main-group light element Mg^{2+} ions and alkyne-functionalized tetracarboxylate ligands, shows simultaneously the ligand-based fluorescence and phosphorescence at room temperature.

CP/MOF **1**, $[Mg(H_2EBTC)(DMF)_2]$, crystallizes in the monoclinic space group *C2/c* with the formula of $C_{24}H_{22}MgN_2O_{10}$. As shown in Fig. 1a, the asymmetric unit consists of one half of Mg^{2+} ion and half H_2EBTC^{2-} ligand together with one coordinated DMF molecule. The Mg^{2+} ion occupies the Wyckoff position 4e; the H_2EBTC^{2-} ligand has a centrosymmetric structure and the inversion center is located at the midpoint of the C≡C triple bond. The Mg^{2+} ion has an octahedral coordination atmosphere, in which four of six coordinated oxygen atoms come from four η^1-CO_2^- groups of H_2EBTC^{2-} ligands and other two coordinated oxygen atoms are from two terminal DMF molecules, which remain *cis*

---

[a] *State Key Laboratory of Materials-Oriented Chemical Engineering and College of Chemistry & Molecular Engineering, Nanjing Tech University, Nanjing 210009, P. R. China. E-mail: xmren@njtech.edu.cn.*

[b] *State Key Laboratory of Coordination Chemistry, School of Chemistry and Chemical Engineering, Nanjing University, Nanjing 210023 P. R. China. E-mail: wwzhang@nju.edu.cn.*

[c] *College of Materials Science & Engineering, Nanjing Tech University, Nanjing 210009, P. R. China.*

† Electronic Supplementary Information (ESI) available: Experimental details, PXRD, IR, TG, Uv-vis and PL spectra. CCDC: 1441925 See DOI: 10.1039/x0xx00000x

coordination sites. The symmetry point group of MgO_6 coordination octahedron is C_2. As summarized in Table S1, the Mg-O bond lengths range from 2.070(18) to 2.102(20) Å, and the O-Mg-O bond angles span from 87.23(10) to 172.43(8)°, all of which are comparable to the reported MgO_6 complexes.[16, 17] For the tetracarboxylate H_2EBTC^{2-} ligand, its two phenyl rings are almost coplanar.

Each Mg^{2+} ion is connected to its four neighboring Mg^{2+} ions by four H_2EBTC^{2-} ligands (ref. Fig. 1b), and each H_2EBTC^{2-} anion serves as a μ_4-bridge ligand to link four Mg^{2+} ions (ref. Fig. S1 in ESI). Such building units are repeated to form a three-dimensional (3-D) network with the terminal disorder DMF molecules situated inside the cavities (ref. Fig. 1c). The window of channels in the framework is approximately 8.9×10.7 $Å^2$ (including van der Waals radii) and the solvent-accessible volume is ca.41.2% calculated by PLATON/SOLV[18] when the coordinated DMF molecules are removed (Fig. S2 in ESI).

From the viewpoint of topology, each H_2EBTC^{2-} ligand provides four donor sites and connects four Mg^{2+} ions, and each Mg^{2+} ion connects four H_2EBTC^{2-} ligands, without considering the terminal ligand DMF molecules, the 3-D structure of **1** can be described as a (4, 4)-connected network with Schläfli symbol of $\{3^{21}\}\{3^{24}\cdot 45^{8}\cdot 6^{12}\}$ when each Mg^{2+} unit and the H_2EBTC^{2-} ligand are respectively reduced as a 4-connected node by TOPOS software (Fig. 1d).[19]

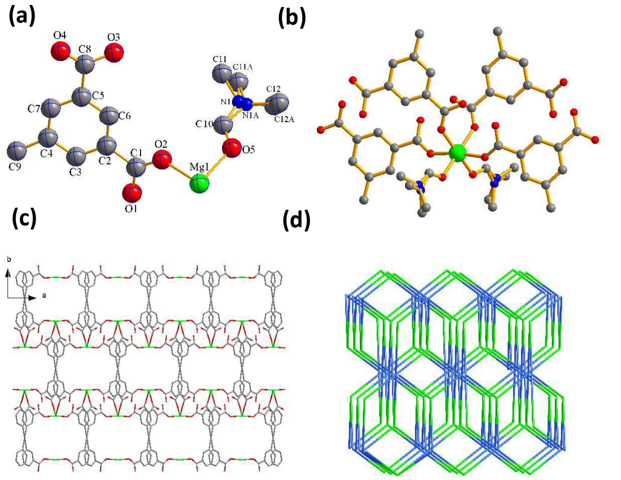

Fig. 1 (a) An asymmetric unit of **1** with thermal ellipsoids at 50% probability level (b) the coordination environment of Mg^{2+} ion (c) representation of 3-D framework viewed along the c-axis (d) (4, 4)-connected network, where the bright green represents the 4-connected node of Mg unit and light blue represents the 4-connected node of organic ligand in **1** (all H atoms were omitted for clarity).

As shown in Fig. S3a and 3b, albeit the phenyl rings of H_2EBTC^{2-} ligands are almost parallel to the (101) crystallographic plane, the offset face-to-face phenyl rings results in so longer centroid-to-centroid distance (4.05 Å) that there is almost no π···π interactions between the phenyl rings of neighboring ligands.

The diffuse-reflectance UV-vis spectra are shown in Fig. S7 (ESI†), indicating that the H_4EBTC exhibits strong absorption in the range of 200-400 nm with a maximum at 322 nm, which may be assigned to the intraligand $\pi\rightarrow\pi^*$ transition of the aromatic rings, and the absorption profiles of **1** is quite similar to that of H_4EBTC. The quite similarity between the UV-vis spectra of H_4EBTC and **1** disclosed that the electronic states of the H_4EBTC ligand is little affected when it is coordinated to the alkaline earth metal ion.[20]

The solid-state emission spectra of H_4EBTC and **1** were further investigated for the powdered samples at room temperature. As depicted in Fig. S8 (ESI†), the H_4EBTC ligand exhibits only a weak emission band with a maximum at 392 nm upon excitation using the light with λ = 278 nm, this emission is attributed to the intraligand π-π^* transition. In contrast to the emission of H_4EBTC, upon excitation at 278 nm, the emission spectrum of **1** showed an intense high-energy (HE) band centered at 376 nm, together with a broad and weak lower-energy (LE) emission band located at around 555 nm (see Fig. 2a). Similar results were obtained when the powdered sample of **1** was excited at 323 nm. The emission lifetime of the HE band is so short that cannot be determined at the present stage owing to the instrument limited, whereas the emission lifetime of the LE band at room temperature can be characterized by single exponential curves (Fig. 2b), and the fit for the decay curve gave the emission decay time of τ = 1.63 μs. In addition, the LE band displays the large Stokes shifts regarding the HE band, as a result, we assign the LE band to the phosphorescence emission and the HE band to the fluorescence emission from the intraligand π-π^* transition. It is interesting that the metal-organic-framework formation of H_2EBTC^{2-} with Mg^{2+} ions not only leads to the fluorescent emission of ligand enhancing, but also triggers the phosphorescent emission of ligand. To the best of our knowledge, no example is described in which the metal ion coordination switches on phosphorescence of an organic chromophore which is not directly involved in metal ion coordination.[21]

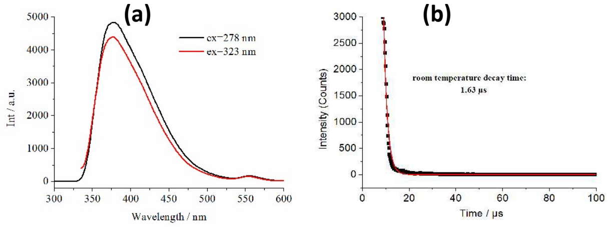

Fig. 2 (a) Solid-state emission spectra of **1** at room temperature by varying the excitation wavelength at 278 nm (black) and 323 nm (red) (b) emission decay of **1** obtained at room temperature upon pulsed excitation at 278 nm and the main emission peaks at 555 nm. The red lines represents the fitting curves and the black squares are the raw experimental data.

Generally, the intensity of luminescence is strongly affected by temperature, and thus, the variable temperature emitting spectra in the solid state were investigated for **1**, as shown in Fig. 3, the temperatures range from 10 to 300 K. Upon cooling, the intensities of both HE and LE emission bands increase simultaneously, this is due to the fact that the thermal activation of non-radiative relaxation process is much reduced at low temperature. The HE and LE bands show different temperature-dependent emission behavior (ref. Fig. 3c and 3d). With respect to the LE band intensity drastically increasing, the HE band intensity increases gradually upon cooling. The emission intensity increases by 3 times for the LE band versus 1.5 times for the HE band when the sample was cooled down from 300 to 10 K. Besides, the peak maximum of the HE band is blue shifted by 10 nm, while the LE peak maximum is red shifted by 6 nm from 300 to 10 K.

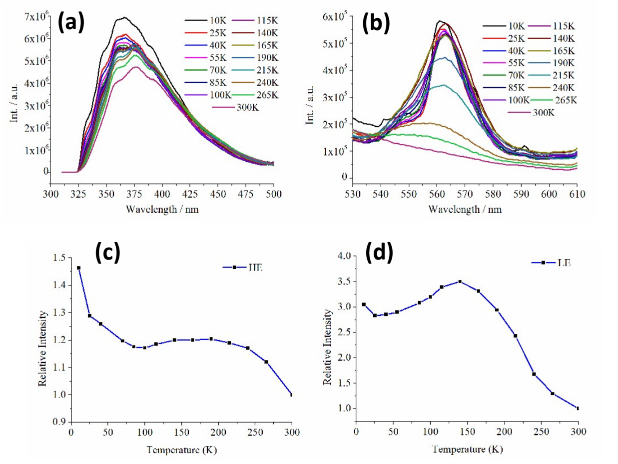

Fig. 3 (a) Temperature-dependent (10-300 K) solid-state luminescence spectra of **1** at 376 nm and (b) 555 nm (ex = 278 nm) and plots showing the changing tendency of the relative intensity of (c) the HE band and (d) the LE band upon temperature (10-300 K).

Generally, the excitation of a conjugated organic molecule to its singlet excited state (S_1) is followed by the triplet state (T_1) through an intersystem crossing process that relaxes to the ground state by phosphorescence. Since the excitation to a triplet state involves an additional "forbidden" spin transition, it is less probable that a triplet state will form when the molecule absorbs radiation. The intersystem crossing process occurring is more favorable when the vibrational levels of two excited states overlap, since little or no energy must be gained or lost in the transition; or as the spin-orbit coupling in a molecule is substantial and a change in spin is thus more favorable, as a result, the intersystem crossing is most common in heavy-atom molecules (e.g. those containing iodine, bromine or coordinated to the heavy metal atom), and very rare in light-atom molecules (only containing C, H and N atoms etc.). In addition, the presence of paramagnetic species in solution also enhances intersystem crossing.

Since the H_4EBTC did not emit phosphorescence, the Mg^{2+} ion coordination switches on phosphorescence of an organic chromophore in **1** at ambient temperature, indicating that the coordination of Mg^{2+} ion to H_4EBTC must be allowing more efficient intersystem crossing from the first excited singlet state to the first triplet state. In addition, CP/MOF **1** is only comprised of light and close-shell atoms of C, H, N, O and Mg, it is impossible that the heavy atom effect or paramagnetic species cooperates to the intersystem crossing process. Thus the efficient intersystem crossing process occurring in **1** is related to the vibrational levels of the excited singlet and triplet states overlap.

In summary, a highly thermal stable CP/MOF comprised of Mg^{2+} and H_2EBTC^{2-} has been achieved and the dual fluorescent and phosphorescent emissions were simultaneously observed at room temperature, which arise from the excited singlet and triplet states located at the ligand relaxing to the ground state. The phosphorescent emission is related to the overlap of vibrational levels of the excited singlet and triplet states in this CP/MOF. This finding might provide a strategy for design of new phosphorescent CPs/MOFs, which are probably applied in the practical phosphorescence-emitting devices.

Authors thank the Priority Academic Program Development of Jiangsu Higher Education Institutions, Special Research Found for the Doctoral Program of Higher Education and the National Nature Science Foundation of China (grant no. 20123221110013, 51173075 and 21271103) for financial support.

References

1 (a) O. M. Yaghi, M. O' Keeffe, N. W. Ockwig, H. K. Chae, M. Eddaoudi, J. Kim, *Nature.* 2003, **423**, 705; (b) K. Takahashi, N. Hoshino, T. Takeda, S.-i. Noro, T. Nakamura, S. Takeda, T. Akutagawa, *Dalton Trans.,* 2014, **43**, 9081.
2 (a) H. W. Hou, L. X. Xie, G. Li, T. Z. Ge, Y. T. Fan, Y. Zhu, *New. J. Chem.,* 2004, **28**, 191; (b) B. Xiao, H. W. Hou, Y. T. Fan, *J. Organomet Chem.* 2007, **692**, 2014; (c) P. Y. Wu, C. He, J. Wang, X. J. Peng, X. Z. Li, Y. L. An and C. Y. Duan, *J. Am. Chem. Soc.,* 2012, **134**, 14991; (d) D. B. Dang, P. Y. Wu, C. He, Z. Xie and C. Y. Duan, *J. Am. Chem. Soc.,* 2010, **132**, 14321.
3 (a) H. W. Hou, Y. L. Wei, Y. L. Song, L. W. Mi, M. S. Tang, L. K. Li and Y. T. Fan, *Angew. Chem. Int. Ed.* 2005, **44**, 6067; (b) H. Y. Han, Y. L. Song, H. W. Hou, Y. T. Fan and Y. Zhu, *Dalton Trans.,* 2006, 1972.
4 (a) X. Y. Dong, R. Wang, J. B. Li, S. Q. Zang, H. W. Hou and T. C. W. Mak, *Chem. Commun.,* 2013, **49**, 10590; (b) R. Wang, X. Y. Dong, H. Xu, R. B. Pei, M. L. Ma, S. Q. Zang, H. W. Hou and T. C. W. Mak, *Chem. Commun.,* 2014, **50**, 9153.
5 (a) Y. J. Cui, F. L. Zhu, B. L. Chen and G. D. Qian, *Chem. Commun.,* 2015, **51**, 7420; (b) Y. J. Cui, R. J. Song, J. C.Yu, M. Liu, Z. Q. Wang, C. D. Wu, Y. Yang, Z. Y. Wang, B. L. Chen, G. D. Qian, *Adv. Mater.,* 2015, **27**, 1420.
6 (a) B. Li, H.-M. Wen, Y. J. Cui, G. D. Qian, B. L. Chen, *Prog Polym Sci.,* 2015, **48**, 40; (b) C. X. Tian, L. P. Zhu, F. Lin and S. G. Boyes, *ACS Appl. Mater. Interfaces,* 2015, **7**, 17765.
7 (a) M. A. Baldo, M. E. Thompson and S. R. Forrest, *Nature,* 2000, **403**, 750; (b) C. Wu, H. F. Chen, K. T. Wong and M. E. Thompson, *J. Am. Chem. Soc.*, 2010, **132**, 3133; (c) P. T. Chou and Y. Chi, *Chem.-Eur. J.,* 2007, **13**, 380; (d) K. Zhang, Z. Chen, C. L. Yang, Y. T. Tao, Y. Zou, J. G. Qin and Y. Cao, *J. Mater. Chem.,* 2008, **18,** 291.
8 (a) H. J. Bolink, L. Cappelli, E. Coronado, M. Graetzel, E. Orti, R. D. Costa, P. M. Viruela and M. K. Nazeeruddin, *J. Am. Chem. Soc.,* 2006, **128**, 14786; (b) H. C. Su, F. C. Fang, T. Y. Hwu, H. H. Hsieh, H. F. Chen, G. H. Lee, S. M. Peng, K. T. Wong and C. C. Wu, *Adv. Funct. Mater.,* 2007, **17**, 1019.
9 (a) T. H. Kwon, J. Kwon and J. I. Hong, *J. Am. Chem. Soc.,* 2008, **130**, 3726; (b) D. L. Ma, W. L. Wong, W. H. Chung, F. Y. Chan, P. K. So, T. S. Lai, Z. Y. Zhou, Y. C. Leung and K. Y. Wong, *Angew. Chem., Int. Ed.,* 2008, **47**, 3735.

10 (a) Q. Zhao, F. Y. Li and C. H. Huang, *Chem. Soc. Rev.,* 2010, **39**, 3007; (b) M. Schmittel and H. Lin, *Inorg. Chem.,* 2007, **46**, 9139.
11 (a) F. Geist, A. Jackel and R. F. Winter, *Inorg. Chem.,* 2015, **54**, 10946; (b) W. H. Wu, J. F. Sun, S. M. Ji, W. T. Wu, J. Z. Zhao and H. M. Guo, *Dalton Trans.,* 2011, **40**, 11550.
12 M. Starck, P. Kadjane, E. Bois, B. Darbouret, A. Incamps, R. Ziessel and L. J. Charbonnière, *Chem. Eur. J.* 2011, **17**, 9164.
13 (a) W. H. Wu, J. F. Sun, X. N. Cui and J. Z. Zhao, *J. Mater. Chem. C,* 2013, **1**, 4577; (b) C.-Y. Sun, W.-P. To, X.-L. Wang, K.-T. Chan, Z.-M. Su and C.-M. Che, *Chem. Sci.,* 2015, **6**, 7105.
14 (a) Q. Zhao, L. Li, F. Y. Li, M. X. Yu, Z. P. Liu, T. Yi and C. H. Huang, *Chem. Commun.,* 2008, 685; (b) K. W. Huang, H. Z. Wu, M. Shi, F. Y. Li, T. Yi and C. H. Huang, *Chem. Commun.,* 2009, 1243.
15 D. J. Lewis, F. Moretta, A. T. Holloway and Z. Pikramenou, *Dalton Trans.,* 2012, **41**, 13138.
16 L. Zhai, W. W. Zhang, J. L. Zuo, X. M. Ren, *Dalton Trans.* 2016, **45**, 3372.
17 (a) K. L. Gurunatha, K. Uemura and T. K. Maji, *Inorg. Chem.*, 2008, **47**, 6578; (b) R. Sen, D. Saha and S. Koner, *Chem.-Eur. J.,* 2012, **18**, 5979.
18 A. L. Spek, *J. Appl. Crystallogr.,* 2003, **36**, 7.
19 V. A. Blatov, A. P. Shevchenko and V. N. Serezhkin, *J. Appl. Crystallogr.,* 2000, **33**, 1193.
20 A. Douvali, A. C. Tsipis, S. V. Eliseeva, S. Petoud, G. S. Papaefstathiou, C. D. Malliakas, I. Papadas, G. S. Armatas, I. Margiolaki, M. G. Kanatzidis, T. Lazarides, M. J. Manos, *Angew. Chem., Int. Ed*. 2015, **54**, 1651.
21 A. Fermi, G. Bergamini, M. Roy, M. Gingras, P. Ceroni, *J. Am. Chem. Soc.* 2014, **136**, 6395.